

Receding horizon viability radius for stability of humanoid robot under external perturbation[†]

Sangyong Lee¹, Munsang Kim^{2,*}, Jongwon Kim³ and Mun-Taek Choi⁴

¹*School of Mechanical and Aerospace Engineering, Seoul National University, Seoul, 151-742, Korea*

²*Center for Intelligent Robotics, Korea Institute of Science and Technology,
39-1 Hawolgok-dong, Sungbuk-gu, Seoul 136-791, Korea*

³*Mechanical and Aerospace Engineering, Seoul National University, Seoul, 151-742, Korea*

⁴*Center for Intelligent Robotics, Korea Institute of Science and Technology,
39-1 Hawolgok-dong, Sungbuk-gu, Seoul 136-791, Korea*

(Manuscript Received March 24, 2009; Revised March 2, 2010; Accepted March 8, 2010)

Abstract

In this paper, a new approach that uses the rate of change of the angular momentum about the center of mass (COM) to improve the balance of a humanoid robot is proposed. This approach is motivated by how humans balance themselves when standing, walking, and running by making use of their upper body and swinging legs. Human movements such as lunging forward or backward and rotating arms make use of angular momentum to maintain balance. As the external perturbation increases, a human instinctively decides when and where to take a step to avoid a fall. In the same manner, a humanoid robot subjected to an external perturbation can determine whether to remain standing or to take a step with a swinging leg to maintain balance using RHVR conditions obtained from the proposed linear inverted dumbbell model. The rotation of a dumbbell model with mass inertia is an easy expression of the angular momentum of an upper body, arms, and legs. A zero-moment point (ZMP) outside the support polygon indicates an unbalanced gait and cannot represent a physical point related to the sole of the robot foot, which is defined as pseudo-ZMP (PZMP) in this paper. PZMP located outside the support area provides useful information for balancing the gait. PZMP from the foot edge provides a measure of the unbalanced moment that tends to rotate the humanoid robot around the supporting foot and causes it to fall. It is shown that PZMP is determined by the Gauss's principle within mechanical constraints of the rate of change of angular momentum about COM. In fact, the actual angular acceleration about COM is determined by the Gauss's principle. Additionally, RHVRs is defined, that is, viability regions to keep the balance that indicate the essential range of stability implemented to a real system. RHVRs are divided into the real ZMP (RZMP), PZMP and stepping PZMP (SPZMP). Hence, the regions of RHVR and the actual angular acceleration about COM determine which of the three control strategies is used.

Keywords: Linear inverted dumbbell model; Receding horizon viability radius; Pseudo-zmp; Gauss's principle

1. Introduction

Humans are capable of performing numerous dynamical movements in a wide variety of complex and novel environments while robustly rejecting a large spectrum of disturbances. Human movements such as a forward lunge and rapid arm rotations make use of angular momentum to maintain overall balance. Many researchers have studied humanoid robots as a way to understand humans. It is difficult to use a general approach for studying the stability of a humanoid robot under an external disturbance. To deal with small disturbances, it may be sufficient for a robot to simply behave as an

inverted pendulum with a compensating torque at the ankle [1]. As the disturbance increases, the robot must use more of its upper body and swing its legs. Bending of the hips or swinging of the legs compensates additional torques due to larger disturbances. If the disturbance is too large, the robot can avoid falling only by taking a step. However, simplified models of a humanoid robot, such as the linear inverted pendulum model (LIPM) developed by Kajita [2], do not consider rotational inertia, and therefore, they cannot capture this behavior. The LIPM is linearized about the vertical and constrained to a horizontal plane. An extension of the LIPM is the linear inverted pendulum plus flywheel model developed by Pratt et al. [3]. This model achieves control and stability of a humanoid robot by simply using meaningful velocity formulations. The velocity-based formulations are used to determine the capture region into which the humanoid robot must step to avoid fall-

[†] This paper was recommended for publication in revised form by Associate Editor Jong Hyeon Park

*Corresponding author. Tel.: +82 2 958 5623, Fax.: +82 2 958 6989

E-mail address: munsang@kist.re.kr

© KSME & Springer 2010

ling. Occasionally, the capture region may be outside the robot's range of motion and it must therefore take more than one step to balance itself. A disadvantage of this model is that it does not consider the effect of ankle torque. However, it appears that the angular momenta about the center of pressure (COP) and center of mass (COM) are important factors that must be controlled.

The rotation equilibrium of the foot is an important criterion for the evaluation and control of the gait and postural stability in a humanoid robot. Goswami [4] proposed the foot rotation indicator (FRI), which indicates the unbalanced torque acting only during the single-support phase of a humanoid robot. He also proposed the zero rate of change in angular momentum (ZRAM) point [5], which is a useful criterion for the analysis and control of the balance of a humanoid robot in very general situations. Unlike the FRI, the ZRAM point is not defined on the basis of physical rotation of the foot and is valid during both the single- and double-support phases. However, ZRAM cannot be applied in a practical system due to theoretically physical quantity without kinematic consideration of a humanoid robot. Popovic et al. [6] proposed the use of the zero-spin angular momentum instead of the COM torque. If the spin angular momentum motivated by biomechanical findings is not precisely regulated, the actual COP will obviously differ from the zero-spin COP (ZSCOP). Assuming the ground reaction force (GRF) to be sufficiently large, the zero-spin COP moves outside the foot support polygon. When there is a large and rapid turning motion such as a nonzero vertical torque, the ZSCOP shifts from the actual one. Essentially, however, the ZSCOP, ZRAM, and centroidal moment pivot (CMP) all coincide. However, they cannot be practically applied to a humanoid robot under external perturbation.

Obviously, a loss of balance implies that the rate of change of angular momentum about the COM is nonzero. When a humanoid robot has an overall nonzero angular momentum, it tips, and this results in either spinning or falling. Even a humanoid robot having a constant nonzero angular momentum can fall. If the resultant external moment on the humanoid robot is zero, then the overall rate of change of angular momentum is zero and overall rotational stability or equilibrium is achieved. However, it is practically difficult to achieve this state since it is infeasible to make the rate of change of angular momentum about the COM zero.

Thus, we first describe how to minimize the rate of change of angular momentum about the COM within mechanical constraints and then present viability regions to achieve balancing posture strategies of a humanoid robot under various external perturbations.

The zero-moment point (ZMP) coincides with the COP when within the support polygon (called the real ZMP or RZMP); however, when it is outside the support polygon, it is called the pseudo-ZMP (PZMP), which is obtained to minimize the rate of change of angular momentum about the COM. However, it is practically difficult to measure the rate of change of angular momentum about the COM. Nonetheless,

determining the same is very important for achieving stability of a humanoid robot.

We describe how to solve this problem using the Gauss's principle, which expresses an extreme property of the real motion of a system in the class of admissible motions and defines the viability regions as the receding horizon viability radius (RHVR), which indicates the essential range of the stability implemented in a real system. The RHVRs are divided into the real ZMP (RZMP), PZMP and stepping PZMP (SPZMP).

In section 2, a linear inverted dumbbell model (LIDM) that approximates the rate of change of angular momentum about the COM is described. This model has the advantage of approximating the behavior of the upper body or swinging leg in a humanoid robot. In section 3, the PZMP is shown as a more practical criterion for the stability of a humanoid robot as compared to other criteria such as the COP, FRI, and CMP. Section 4 describes how to obtain the PZMP. The RHVR, which is considered for three different cases, is summarized in section 5, and the conclusions are presented in section 6.

2. Linear inverted dumbbell model

The resultant external moment on a body equals the rate of change in the body's angular momentum. If this moment is defined relative to the body's COM, then the angular momentum is known as the central angular momentum. If G denotes the body's COM and H_G denotes the body's central angular momentum, then \dot{H}_G denotes the rate of change in the body's central angular momentum. A humanoid robot's \dot{H}_G can be used to maintain or improve the robot's balance. If \dot{H}_G is zero, then overall rotational stability has been achieved. The ZRAM point is the point on the foot/ground surface where the total GRF would have to act such that the rate of change in angular momentum is zero [5]. When the humanoid robot is subjected to a resultant GRF acting at the COP, the COP is within the support polygon and the GRF passes through the COM. At this instant, the humanoid robot is rotationally stable. However, when the GRF generates a net nonzero moment about the COM, the humanoid robot tends to fall. If the GRF shifts parallel to the line passing through the COM, the point at which the rate of change of angular momentum reduces to zero and the humanoid robot becomes stable is defined by ZRAM. However, since ZRAM is a theoretical point that does not consider the kinematic constraints of a system, the PZMP, which does consider these constraints, is used in this paper.

This section introduces the LIDM for the approximation of angular momentum. The equation of motion for the free dynamics of the LIDM in a central gravitational field describes the translational or rotational dynamics. The LIDM is assumed to remain within a fixed orbital plane. It consists of two ideal masses connected by a linear rigid rod that is assumed to be massless. The dumbbell body can rotate and translate within a plane. A gravitational force acts on each individual mass.

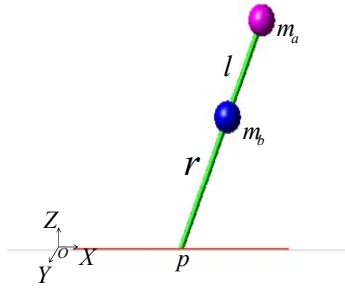


Fig. 1. Linear inverted dumbbell model with zero \dot{H}_G .

Though the LIDM is an exceedingly simple model, it is effective in demonstrating the complex dynamics and control phenomena of the stability of a humanoid robot. The radial distance of the COM of the dumbbell from point P is denoted by r , and the distance of each mass particle from the COM of the dumbbell is l . ρ denotes the angular position of the dumbbell COM and θ denotes the attitude angle of the dumbbell axis with respect to the radial direction from point P to the dumbbell COM. The dumbbell is free to spin about its midpoint. A pin can be used to lock the dumbbell into the position shown in Fig. 1.

When the pin is withdrawn, the dumbbell is free to rotate about its midpoint, as shown in Fig. 2. The sum of the moments of all external forces must equal the change of angular momentum of the dumbbell. Since the dumbbell is symmetric, the COM is at the support point. The angular momentum of the dumbbell with respect to point P is

$$H_p = \sum_{i=1}^2 r_i \times \left(\frac{m}{2} v_i\right) = \sum_{i=1}^2 (r_G + l_i) \frac{m}{2} v_i = m r_G \times \dot{r}_G + H_G \quad (1)$$

where H_G is the angular momentum of the dumbbell with respect to the COM G . The parallel axis theorem gives

$$H_G = \sum_{i=1}^2 l_i \times \frac{m}{2} (\dot{\theta}_G \times l_i) \quad (2)$$

where $m = 2m_a = 2m_b$ and $\dot{\theta}_G$ is the angular velocity of the dumbbell.

$$H_G = l \frac{m}{2} l \dot{\theta}_G + l \frac{m}{2} l \dot{\theta}_G = m l^2 \dot{\theta}_G \quad (3)$$

If the pin is locked, then H_G is constant:

$$H_p = r_G \times m \dot{r}_G = m(l^2 + r^2) \dot{\rho}_o \quad (4)$$

The rate of change in the angular momentum of the dumbbell with respect to point P is

$$\dot{H}_p = r_G \times m \ddot{r}_G \quad (5)$$

$$OP \times R_z + OG \times mg = OG \times m a_G \quad (6)$$

where $OP = [p_x, p_y, 0]^T$, $OG = [x_G, y_G, z_G]^T$, $g = [0, 0, -g]^T$,

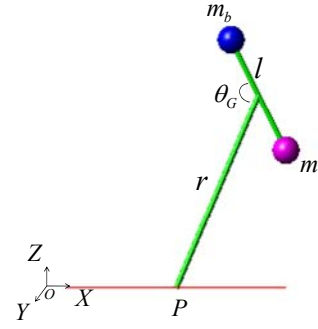


Fig. 2. Linear inverted dumbbell model with non-zero \dot{H}_G .

and R_z is the GRF. Let the x-component of the ZMP be p_x . Then,

$$m p_x (\ddot{z}_G + g) + m x_G g = m z_G \ddot{x}_G - m x_G \ddot{z}_G \quad (7)$$

$$m p_x (\ddot{z}_G + g) = m z_G \ddot{x}_G - m x_G (\ddot{z}_G + g) \quad (8)$$

$$\therefore p_x = x_G - \frac{z_G}{(\ddot{z}_G + g)} \ddot{x}_G \quad (9)$$

We assume $\ddot{z}_G = 0$.

$$\therefore p_x = x_G - \frac{z_G}{g} \ddot{x}_G \quad (10)$$

The y-component of the ZMP can be found in a similar manner.

If the pin is unlocked, then $H_p = H_G + r_G \times m \dot{r}_G$

$$H_o = H_G + OG \times m \dot{r}_G \quad (11)$$

$$\dot{H}_o = \dot{H}_G + OG \times m \ddot{r}_G \quad (12)$$

$$m p_x (\ddot{z}_G + g) = \pm m l^2 \ddot{\theta}_G + m x_G (\ddot{z}_G + g) - m \ddot{x}_G z_G \quad (13)$$

$$\therefore p_x = x_G - \frac{z_G}{(\ddot{z}_G + g)} \ddot{x}_G \pm \frac{l^2}{(\ddot{z}_G + g)} \ddot{\theta}_G \quad (14)$$

We assume $\dot{z}_G = 0$, $\ddot{z}_G = 0$

$$\therefore p_x = x_G - \frac{z_G}{g} \ddot{x}_G \pm \frac{l^2}{g} \ddot{\theta}_G \quad (15)$$

The y-component of the ZMP can be found in a similar manner. When the ZMP lies outside the support polygon, the points on the ground surface at which the total GRF would have to act such that the rate of change in angular momentum is zero can be defined as the PZMP.

The PZMP for the total angular momentum can be calculated using Eq. (15). The total angular momentum is the sum of the angular momenta about the COM and about the COP. The angular momentum is a conserved physical quantity for isolated systems in which no external moment acts on the COM. However, when the body is subjected to external perturbations, the conservation of the whole-body angular momentum cannot be guaranteed. In this case, the calculated ZMP does not represent the RZMP but a hypothetical point at which the ZMP would be if the support polygon was large enough to encompass it. As this is not the real case, the calcu-

lated ZMP is outside the support polygon and the point is called the PZMP; the PZMP represents the occurrence of a perturbation moment and the beginning of the rotation of the humanoid robot as a whole about the foot edge. The distance from the FEP to the PZMP is proportional to the intensity of the perturbation moment. The minimum distance from the FEP to the PZMP can be obtained from the Gauss's principle, which minimizes the Gaussian of the total angular momentum. During the flight phase of running or jumping, angular momentum is perfectly conserved since the dominant external force is gravity acting at the body's COM. However, during the support phase of walking, angular momentum is not necessarily constant because the legs can exert forces on the ground that tends to accelerate the robot. Hence, the humanoid robot should modulate moments about the COM to control the change of angular momentum and whole-body angular excursions. Consequently, the regulation of the angular momentum about the COM is critical for the stability of the humanoid robot.

3. Comparison with other dynamic equilibrium criterions

3.1 Zero-moment point/Center of pressure

The notion of the ZMP for a humanoid robot has been known for more than 30 years, and the ZMP is a significant dynamic equilibrium criterion as long as gravitational forces govern the balancing of the gait. The overall balancing indicator of humanoid robot behavior is the point at which the influence of all forces acting on the robot can be replaced by a single force. Vukobratovic [7] defined the ZMP as the point at which pressure under the supporting foot can be replaced by the GRF acting on the sole of the robot foot. The term "zero-moment point" refers to the point at which the x- and y-components of the moment replacing the active forces are zero, with only a nonzero vertical component being permitted.

In the single-support phase in which only one foot is in contact with the ground while the other is in a swing phase, the support polygon, that is, the area within the convex hull of the foot support area, is identical to the foot surface. In the double-support phase in which two feet are in contact with the ground, the support polygon is defined by the foot surfaces and the distance between them. The COP represents the point on the support foot at which the resultant of the distributed GRFs acts. Alternatively, the field of pressure forces is equivalent to a single resultant force and it is exerted at the point at which the resultant moment is zero [8]. In general, the pressure between the robot foot sole and the ground can be replaced by the force acting at the COP on the humanoid robot during gait. If the humanoid robot has a dynamically balanced gait, the COP and ZMP on the foot surface are identical. However, the ZMP has a more specific meaning than the COP does in evaluating the dynamics of the gait equilibrium. To illustrate the specific difference between the ZMP and COP, if the ZMP lies on the edge of the support polygon, the trajectory may not be dy-

namically feasible. The perturbation moment causes rotation of the complete humanoid robot about the edge point. In spite of the COP and ZMP coinciding on the edge of the support polygon, a humanoid robot rotating about a foot edge becomes unstable and falls. When the ZMP lies outside the support polygon under a more critical perturbation, the RZMP does not exist. Otherwise, the COP exists at the foot edge point on the support foot at which the resultant of distributed GRFs acts. Consequently, in this unbalanced situation, the ZMP does not coincide with the COP. The ZMP being outside the support polygon indicates an unbalanced gait and does not represent a physical point related to the sole of the robot foot. The point outside the support polygon is defined as the PZMP in section 2. The distance of the PZMP from the foot edge provides a measure of the unbalanced moment that tends to rotate the humanoid robot around the supporting foot and causes it to fall. The measure depends on the intensity of the perturbation moment limited by the kinematic constraint of a dumbbell. To avoid overturning, rapid rebalancing by changing the dynamic forces acting on the body is required.

3.2 Foot rotation indicator

The FRI point, which is a point on the foot/ground contact surface within or outside the support polygon, is where the net GRF would have to act to maintain a zero-moment condition about the foot [4]. Foot rotation in a humanoid robot during the single-support phase is an indication of postural stability. The rotational dynamic equilibrium of the foot is therefore an important criterion for the control strategy of postural stability in a humanoid robot. The external forces that cause foot rotation are the resultant ground force, moment at the COP, and gravity. Hence, the rotational dynamic equilibrium can be obtained by the summation of external moments acting on the humanoid robot. The FRI point is applicable only during the single-support phase of the humanoid robot. To ensure no foot rotation, the FRI point must remain within the convex hull of the foot support area. This condition is identical to the definition of the RZMP. However, the RZMP may not lie outside the support polygon, whereas the FRI point does so whenever there is an unbalanced torque on the foot. Thus, the FRI point indicates the stability margin of the humanoid robot during the single-support phase. As stated above, however, this distance is equivalent to the definition of the PZMP, which provides a measure of the unbalanced moment that tends to rotate the humanoid robot around the supporting foot and causes it to fall. In addition, the PZMP is applicable for any phase of the humanoid robot and is therefore a more practical consideration than the FRI point for balancing the robot.

In the top fig 3(a), the foot is in static equilibrium since RZMP is coincident with FRI. However, when the foot is starting to rotate in the top fig 3(b), FRI is outside the support polygon but RZMP is at the tip about which the foot rotates. In the bottom fig 3(c), if the foot does not rotate under external perturbation, both PZMP and FRI is outside the support poly-

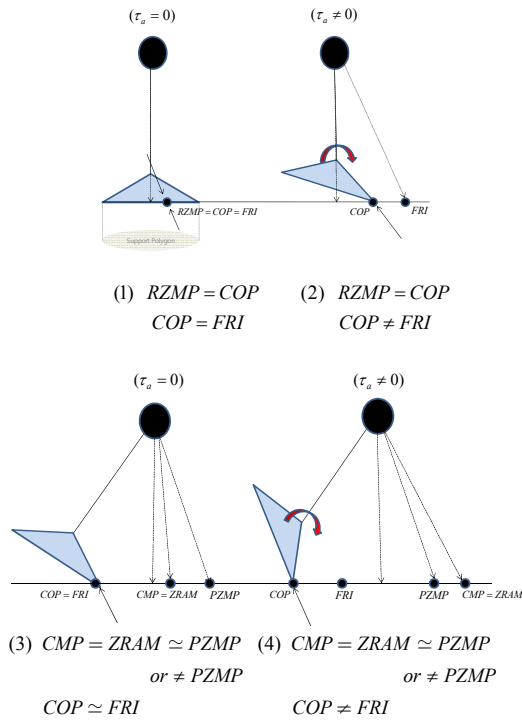


Fig. 3. Dynamic equilibrium criteria.

gon and PZMP is coincide with FRI. Otherwise, if the foot rotates under external perturbation, both PZMP and FRI is outside but PZMP is not coincident with FRI shown as the fig 3(d).

3.3 Centroidal moment pivot

The centroidal moment pivot (CMP) is the point at which the GRF would have to act to keep the horizontal component of the whole-body angular momentum constant [9]. The CMP is defined as the point at which a line parallel to the GRF and passing through the COM intersects with the ground surface. When the moment about the COM is zero, the CMP coincides with the ZMP. When the CMP and the ZMP do not coincide, there exists a nonzero body moment about the COM. While the ZMP cannot lie outside the support polygon, the CMP can, but only in the presence of a significant moment about the COM. The CMP, applicable for both single- and double-support phases, provides information about the whole-body rotational dynamics when supplemented with the ZMP location. When the humanoid robot loses rotational equilibrium, it does not necessarily mean that it will fall. However, Goswami and Kallen (2004) [5] called the specified quantity the ZRAM point. The CMP is thus equivalent to the ZRAM.

A control strategy that minimizes the CMP–ZMP separation would only ensure a constant whole-body angular momentum and not necessarily zero angular momentum. The CMP can be expressed mathematically by requiring that the cross-product of the CMP–COM position vector and the GRF vector vanish [10]. That is,

$$[(\vec{r}_{CMP} - \vec{r}_{COM}) \times \vec{F}]_{horizontal} = 0 \tag{16}$$

The location of the CMP can be written in terms of the location of the COM and the GRF as

$$\begin{aligned} x_{CMP} &= x_{COM} - \frac{F_x}{F_z} z_{COM} \\ y_{CMP} &= y_{COM} - \frac{F_y}{F_z} z_{COM} \end{aligned} \tag{17}$$

where $F_x = m\ddot{x}$, $F_y = m\ddot{y}$, and $F_z = m(\ddot{z}_G + g)$

Eq. (17) is the same as Eq. (10) of the RZMP and does not show us the practical measurement to prevent falling down when the RZMP lies outside the support polygon. On the other hand, the PZMP shows how to measure the essential range for the stability of the humanoid robot under external perturbation.

4. Receding horizon viability radius

4.1 Fundamental equation by Gauss's principle

The Gauss's principle is a basic axiom of physics in a manner similar to Newton's laws of motion. It describes how masses move under the influence of forces and how to take geometric motion constraints into account. The Gauss's principle, established by Gauss [12], expresses an extreme property of the real motion of a system in the class of admissible motions, corresponding to the ideal constraints imposed on the system and to the conditions of constancy of position and velocities of the points in the system at a given instant. Suppose that the Cartesian coordinates and velocities of a system are given at time t . Then, we can write

$$G(\ddot{x}) = \frac{1}{2} \sum_{i=1}^N m_i (\ddot{x}_i - \frac{F_i}{m_i})^2 \tag{18}$$

$G(\ddot{x})$ is a function of the set of accelerations \ddot{x}_i . The Gauss's principle states the actual acceleration corresponds to the minimum value of $G(\ddot{x})$. If the system is not constrained, then $G(\ddot{x})$ is zero and the system evolves under Newton's equation. The Gauss's principle states that the trajectories actually followed are those that deviate as little as possible, in a least squares sense, from the unconstrained Newtonian trajectories. The projection that the system actually follows is one that minimizes the magnitude of the constraint force. This implies that the constraining force must be parallel to the normal of the constraint surface. This is Gauss's principle of least constraint. The postural stability of a humanoid robot subjected to a strong external perturbation is related to the whole-body angular momentum. Hence, the Gauss's principle provides important information about the postural stability of a humanoid robot subjected to a strong external perturbation in predicting the whole-body angular momentum. The Gauss's principle gives a clear description of the general nature of constrained motion in terms of the minimization of a function of the acceleration of a system [11-13]. The Gauss's principle in terms of generalized

coordinates is given by

$$G(\ddot{q}) = [\ddot{q} - a(t)]^T M(q, t) [\ddot{q} - a(t)]. \quad (19)$$

where the matrix M is an $s \times s$ symmetric positive definite matrix and the vector $a(t)$ corresponds to the acceleration at time t of the unconstrained system. \ddot{q} is the actual acceleration vector of the constrained system. The fundamental equation is proved in generalized coordinates. The equation for the unconstrained system is known to always be in the form

$$M(q, t)a(t) = F(q, \dot{q}, t). \quad (20)$$

Here, the generalized force F is the given impressed force acting on the system. The equation of constraint is defined as

$$A(q, \dot{q}, t)\ddot{q} = b(q, \dot{q}, t), \quad (21)$$

The vector q is an s -generalized coordinate q_1, q_2, \dots, q_s since they are independent. If the holonomic constraints v and the non-holonomic constraints u are characterized by the system, there are a total of $w = v + u$ equations. The matrix A is a $w \times s$ matrix, where $i = 1 \dots w$ is the constraint number.

If A is a square nonsingular matrix, then the usual inverse of A , A^{-1} , satisfies all four of the MP conditions (Appendix A).

If A is a positive definite matrix and $w = s$, it can be expressed as

$$\begin{aligned} A^{\frac{1}{2}} &= W \Lambda^{\frac{1}{2}} W^T, \quad A^{-\frac{1}{2}} = W \Lambda^{-\frac{1}{2}} W^T \\ AW &= W \Lambda, \quad W^T W = I, \end{aligned} \quad (22)$$

where W is an orthogonal matrix and Λ is a diagonal matrix. In the absence of constraint Eq. (21), the acceleration $\ddot{q}(t) = a(t)$ of the unconstrained system is given by Eq. (20).

$$a(t) = M^{-1}(q, t)F(q, \dot{q}, t) \quad (23)$$

In general, the matrix A has rank $r \leq w$, where r is the number of row vectors. Additionally, the w constraint equations need not be independent. The acceleration $\ddot{q}(t)$ of the constraint equation at each instant t must satisfy Eq. (21). For clarity, the arguments of various matrices and vectors are suppressed, and the matrix M is assumed to be positive definite. Vector \ddot{r} is defined as

$$\ddot{r}(t) = M^{\frac{1}{2}}(q, t)\ddot{q}(t). \quad (24)$$

Eq. (24) can be substituted into the constraint Eq. (21). The acceleration of the constrained system then satisfies Eq. (25).

$$A(q, t)M^{-\frac{1}{2}}(q, t)\ddot{r}(t) = b(q, \dot{q}, t). \quad (25)$$

$B = AM^{-1/2}$ is defined as a constraint matrix, where B is a $w \times s$ matrix.

$$B(q, t)\ddot{r}(t) = b(q, \dot{q}, t) \quad (26)$$

The general solution to the constraint equation $AX = b$ can be expressed by

$$X = A^+b + (I - A^+A)h \quad (27)$$

where A is an $m \times n$ matrix and h is any $n \times 1$ vector. (Appendix B). In the same sense, the general solution to Eq. (26) is simple.

$$\ddot{r}(t) = B^+b + (I - B^+B)h \quad (28)$$

Here, B^+ is the $s \times w$ Moore–Penrose inverse of matrix B , and h is an arbitrary $n \times 1$ vector. Eq. (28) can be rewritten as

$$\ddot{r}(t) = B^+b + Rh \quad \text{where, } R = (I - B^+B) \quad (29)$$

The vector Rh needs to be defined in accordance with the Gauss's principle in analytical mechanics. The acceleration of the constrained system must satisfy the constraint equation at time t . Among the accelerations, the Gauss's principle minimizes the constraint that deviates from the acceleration of the constrained system, such as $\Delta\ddot{q}(t) = \ddot{q}(t) - a(t)$. The quantity $G(\ddot{q})$ is the square of the length of the vector $\Delta\ddot{q}(t)$ normalized with respect to the matrix M . If minimized, $G(\ddot{q})$ is given by

$$\begin{aligned} G(\ddot{q}) &= (\ddot{q} - a)^T M (\ddot{q} - a) \\ &= (M^{\frac{1}{2}}\ddot{q} - M^{\frac{1}{2}}a)^T (M^{\frac{1}{2}}\ddot{q} - M^{\frac{1}{2}}a) \\ &= (\ddot{r} - M^{\frac{1}{2}}a)^T (\ddot{r} - M^{\frac{1}{2}}a). \end{aligned} \quad (30)$$

Substituting Eq. (28) into Eq. (30), vector h needs to be found such that Eq. (31) is minimized.

$$G(h) = (Rh - (M^{\frac{1}{2}}a - B^+b))^T (Rh - (M^{\frac{1}{2}}a - B^+b)). \quad (31)$$

Hence, if matrix A is $m \times n$ and b is an $m \times 1$ vector, an $n \times 1$ vector X is minimized by

$$K(x) = \|AX - b\|^2 = (AX - b)^T (AX - b). \quad (32)$$

given that $X = A^+b + (I - A^+A)h$.

Therefore, h is obtained to minimize $G(h)$:

$$h = R^+(M^{\frac{1}{2}}a - B^+b) + (I - R^+R)K. \quad (33)$$

where K is an arbitrary $n \times 1$ vector. Since $R = (I - B^+B)$ is defined, R is obtained from $RR = R, R^+ = R$, to give

$$h = R^+(M^{\frac{1}{2}}a - B^+b) + (I - R)K. \quad (34)$$

Multiplying both sides by R gives

$$\begin{aligned} Rh &= RR^+(M^{\frac{1}{2}}a - B^+b) + R(I - R)K \\ &= RR(M^{\frac{1}{2}}a - B^+b) + (R - RR)K \end{aligned} \quad (35)$$

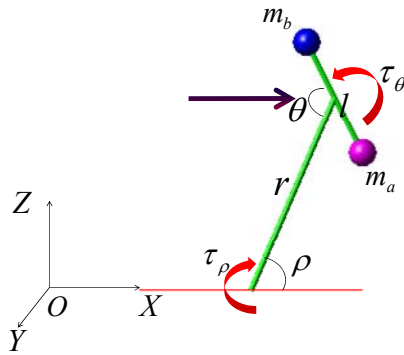


Fig. 4. Dynamic dumbbell system.

$$= R(M^{\frac{1}{2}}a - B^+b).$$

Eq. (35) is substituted into Eq. (29) to give

$$\begin{aligned} \ddot{r}(t) &= B^+b + R(M^{\frac{1}{2}}a - B^+b) \\ &= B^+b + (I - B^+B)(M^{\frac{1}{2}}a - B^+b) \\ &= M^{\frac{1}{2}}a + B^+(b - BM^{\frac{1}{2}}a) \\ &= M^{\frac{1}{2}}a + (AM^{-\frac{1}{2}})^+(b - Aa). \end{aligned} \tag{36}$$

The total acceleration of the constrained system is given by

$$\ddot{q}(t) = a + M^{-\frac{1}{2}}(AM^{-\frac{1}{2}})^+(b - Aa) \tag{37}$$

Both sides of Eq. (37) can be multiplied by M to obtain

$$\begin{aligned} M\ddot{q}(t) &= Ma + M^{\frac{1}{2}}(AM^{-\frac{1}{2}})^+(b - Aa) \\ &= F(t) + F^c(t). \end{aligned} \tag{38}$$

The unconstrained equation is $Ma(t) = F(t)$ and the constrained equation is

$$F^c(t) = M^{\frac{1}{2}}(AM^{-\frac{1}{2}})^+(b - Aa) \tag{39}$$

The actual acceleration of the constrained system is that given by Eq. (37).

4.2 Equation of motion for LIDM

The kinetic and potential energies of the inverted dumbbell system shown in Fig. 4 in terms of the independent coordinates r, ρ , and θ are

$$T = \frac{m}{2}r^2\dot{\rho}^2 + \frac{m}{2}l^2(\dot{\rho} + \dot{\theta})^2 \tag{40}$$

$$V = mgr(\sin \rho - 1) \tag{41}$$

$$L = \frac{m}{2}(\dot{r}^2 + r^2\dot{\rho}^2 + \dot{l}^2 + l^2(\dot{\rho} - \dot{\theta})^2) - mgr(\sin \rho - 1) \tag{42}$$

The equation of motion about the unconstrained system is

$$\underbrace{\begin{bmatrix} ml^2 + mr^2 & ml^2 \\ ml^2 & ml^2 \end{bmatrix}}_M \underbrace{\begin{bmatrix} \dot{\rho} \\ \dot{\theta} \end{bmatrix}}_{\dot{q}} = \underbrace{\begin{bmatrix} mgr \sin \rho + \tau_\rho \\ \tau_\theta \end{bmatrix}}_F \tag{43}$$

If the force is given in terms of rectangular components, the generalized force components are

$$\begin{aligned} F_s &= \sum_{i=1}^2 F_i \frac{\partial u_i}{\partial q_i} \quad s = 1, 2 \\ \tau_\rho &= F_x \frac{\partial x}{\partial \rho} + F_y \frac{\partial y}{\partial \rho} + F_z \frac{\partial z}{\partial \rho} \\ \tau_\theta &= F_x \frac{\partial x}{\partial \theta} + F_y \frac{\partial y}{\partial \theta} + F_z \frac{\partial z}{\partial \theta} \end{aligned} \tag{44}$$

4.2.1 Impulse–momentum relationships

Generally, strong external perturbation acting on a humanoid robot is assumed to be a force that tends to infinity at an isolated instant such that its time integral remains bounded. Physically, an impulsive force is a very large force that acts over a very short time period. Therefore, a strong external perturbation is considered as an impulsive force. Since the mass m of the robot is constant, the linear momentum L of the mass system is $m\dot{x}$. The equation of motion according to Newton’s generalized second law is

$$m\ddot{x} = \sum F \tag{45}$$

Integrating Eq. (45) gives

$$\begin{aligned} m(\dot{x}(t_1) - \dot{x}(t_0)) &= \int_{t_0}^{t_1} \sum F dt \\ \therefore \lim_{t \rightarrow t_1} \int_{t_0}^t F(x, \dot{x}, t) dt &= p_L \end{aligned} \tag{46}$$

Eq. (46) states that the linear impulse on the body during the interval t_2-t_1 equals the corresponding change in the linear momentum. Similarly, the angular impulse is the time integral of the torque applied to a system, usually for a short time. It is equal to the change of angular momentum that it would cause on a free mass acting about a principal axis. Specifically, the angular impulse represents the effect of a moment of force acting on a system at a distance from the COM. The angular impulse about the mass center for all forces acting on the body during the interval t_2-t_1 equals the corresponding change in the angular momentum about the COM.

$$p_\theta = \int_{t_1}^{t_2} M_G dt = \int_{t_1}^{t_2} \dot{H}_G dt = (H_{G2} - H_{G1}) = \Delta H_G \tag{47}$$

Eq. (47) is particularly useful when dealing with impulse forces. In such cases, it is often possible to calculate the integrated effect of a force on a particle without knowing in detail

the actual value of the force as a function of time. The angular momentum of a system of particles about a fixed point is the sum of the angular momentum of the individual particles. From the LIDM, the angular momentum about the COM is given by Eq. (3):

$$H_G = -\frac{m}{2}l^2(\dot{\rho} - \dot{\theta}_G) - \frac{m}{2}l^2(\dot{\rho} - \dot{\theta}_G) = -ml^2(\dot{\rho} - \dot{\theta}_G) \quad (48)$$

Substituting into Eq. (47) gives

$$\int_{t_1}^{t_2} M_G dt = (H_{G_2} - H_{G_1}) = -ml^2(\dot{\rho}_2 - \dot{\theta}_{G_2}) + ml^2(\dot{\rho}_1 - \dot{\theta}_{G_1}) \quad (49)$$

The time variation in H_G for impact problems about the COM G during the interval t_2-t_1 can be written as

$$p_\theta(t+\tau) - p_\theta(t) = \int_t^{t+\tau} M_G dt \quad (50)$$

$$-ml^2(\dot{\rho}_{t_2} - \dot{\theta}_{G_2}) + ml^2(\dot{\rho}_{t_1} - \dot{\theta}_{G_1}) = \int_{t_1}^{t_2} M_G dt \quad (51)$$

Differentiating Eq. (51) with respect to time gives

$$-ml^2(\ddot{\rho}_{t_2} - \ddot{\theta}_{G_2}) + ml^2(\ddot{\rho}_{t_1} - \ddot{\theta}_{G_1}) = \left(\int_{t_1}^{t_2} M_G dt\right)' \quad (52)$$

The Hamiltonian function for a natural system that is holonomic and conservative is

$$H = \sum_{r=1}^3 p_r \dot{q}_r - L = p_r \dot{r} + p_\rho \dot{\rho} + p_\theta \dot{\theta} - L \quad (53)$$

Consequently, Hamilton's equation for θ , which denotes the attitude angle of the dumbbell axis with respect to the radial direction from point P to the dumbbell COM, is

$$\left(\int_{t_1}^{t_2} M_G dt\right)' = \dot{p}_\theta = -\frac{\partial H}{\partial \theta} = 0 \quad (54)$$

Substituting Eq. (54) into Eq. (52) gives

$$\therefore \ddot{\theta}_{G_2} = \ddot{\theta}_{G_1} + \ddot{\rho}_2 - \ddot{\rho}_1 \quad (55)$$

4.2.2 Constraint equation

The constraint equation is then considered. The basic form of the constraint equations is $A(q,t)\ddot{q} = b(q,\dot{q},t)$. The constraint equation of motion described at each instant is expressed as follows.

$$\begin{aligned} r^2 + l^2 + 2rl \cos \theta &= C_1 \\ r^2 + l^2 - 2rl \cos \theta &= C_2 \end{aligned} \quad (56)$$

$$\begin{aligned} (r+l \cos \theta)\ddot{r} - rl \sin \theta \ddot{\theta} - 2\dot{r}\dot{\theta} \sin \theta - r\dot{\theta}^2 \cos \theta + \dot{r}^2 &= 0 \\ (r-l \cos \theta)\ddot{r} + rl \sin \theta \ddot{\theta} + 2\dot{r}\dot{\theta} \sin \theta + r\dot{\theta}^2 \cos \theta + \dot{r}^2 &= 0 \end{aligned} \quad (57)$$

$$\underbrace{\begin{bmatrix} (r+l \cos \theta) & -rl \sin \theta \\ (r-l \cos \theta) & rl \sin \theta \end{bmatrix}}_A \begin{bmatrix} \ddot{r} \\ \ddot{\theta} \end{bmatrix} = \underbrace{\begin{bmatrix} 2\dot{r}\dot{\theta} \sin \theta + r\dot{\theta}^2 \cos \theta - \dot{r}^2 \\ -2\dot{r}\dot{\theta} \sin \theta - r\dot{\theta}^2 \cos \theta - \dot{r}^2 \end{bmatrix}}_b \quad (58)$$

Thus, the motion of the constrained system is described by the equation

$$M(q,t)\ddot{q} = F(q,\dot{q},t) + F^C(q,\dot{q},t) \quad (59)$$

where $F(q,\dot{q},t)$ is the unconstrained force and $F^C(q,\dot{q},t)$, the constrained force. Assuming that the configuration $q(t)$ and the velocities $\dot{q}(t)$ of the constrained system are known and both $q(t)$ and $\dot{q}(t)$ are continuous at time t , the goal is to obtain the generalized acceleration of the constrained system. Of all the possible generalized acceleration vectors $\ddot{q}(t)$ that satisfy the constrained system at time t , the one that minimizes the Gaussian $G(\ddot{x})$ is given by

$$G(\ddot{x}) = \frac{1}{2} \sum_{i=1}^N m_i \left(\ddot{q} - \frac{F_i}{m_i}\right)^2 = (\ddot{q} - a)^T M (\ddot{q} - a) \quad (60)$$

The determination of the second term in Eq. (59) is dictated by the Gauss's principle. The principle states that at each time t , the acceleration of the constrained system must be such that while satisfying the constraint equation at that instant, it minimizes the Gaussian G .

4.2.3 Actual angular acceleration and RHVR

The Gaussian of the angular acceleration of the COM for an angular impulse is

$$G(\ddot{q}_{t_2}) = \frac{1}{2} \sum_{i=1}^N m_i \left(\ddot{q}_{t_2} - \ddot{q}_{t_1} - \frac{F_i}{m_i}\right)^2 \quad (61)$$

$$G(\ddot{q}_{t_2}) = [\ddot{q} - a]^T M(q,t) [\ddot{q} - a] \quad (62)$$

where $\ddot{q} = \ddot{q}_{t_2} - \ddot{q}_{t_1} = [\ddot{\rho}_{t_2} - \ddot{\rho}_{t_1} \quad \ddot{\theta}_{t_2} - \ddot{\theta}_{t_1}]^T$,
 $a = M^{-1}F$

\ddot{q}_{t_2} is the acceleration matrix after the impulse at time t_2 ; \ddot{q}_{t_1} , the acceleration matrix before the impulse at time t_1 ; Finally, the actual acceleration after the impulsive force at any point in the LIDM can be written as

$$\ddot{q}_{t_2} - \ddot{q}_{t_1} = a + M^{-1}A^T (AM^{-1}A^T)^+ (b - Aa) \quad (63)$$

Consequently, after the impulsive force, the ZMP considered for the actual angular acceleration $\ddot{\theta}_{t_2}$ of the generalized coordinate θ component from Eq. (63) is

$$\therefore p_x = x_G - \frac{z_{G_2}}{g} \ddot{x}_G - \frac{l^2}{g} \ddot{\theta}_{t_2} \quad (64)$$

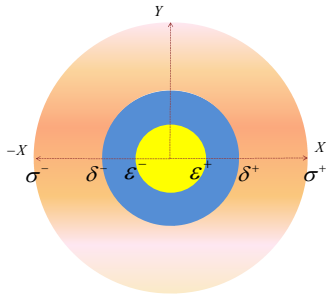


Fig. 5. Ranges of RHVR.

Fig. 5 shows that the RHVR about the RZMP is

$$\varepsilon^- \leq p_x^r \leq \varepsilon^+ \tag{65}$$

ε^- is the minimum RZMP and ε^+ , the maximum RZMP from the center of the ankle. The RHVR about the PZMP is

$$\delta^- \leq p_x^p \leq \delta^+ \tag{66}$$

δ^- is the minimum PZMP and δ^+ , the maximum PZMP. A measure of the unbalanced moment that tends to rotate the humanoid robot around the support foot and cause it to fall is obtained by the distance from ε^- to δ^- or from ε^+ to δ^+ . It must be compensated by the angular momentum of the dumbbell until limit constraints, since the distance is a measure of the instability of the humanoid robot.

The RHVR about the SPZMP is

$$\sigma^- \leq R^s \leq \sigma^+ \tag{67}$$

where σ^- is the minimum SPZMP and σ^+ the maximum SPZMP. The distance from σ^- to σ^+ within the maximum kinematics of the workspace of the swinging leg beyond the joint limits is defined as the maximum viability radius for stepping. The location of the swinging leg for balanced stepping must be the region between σ^- and σ^+ .

5. RHVR control strategies

This section explains how the humanoid robot can maintain or improve its balance in three cases. In the theoretical case, when the rate of change in the angular momentum about the COM is zero under external perturbation, the humanoid robot can prevent falling. However, because this is practically infeasible, the main issue for the stability of the humanoid robot under external perturbation is to greatly minimize the rate of change in the angular momentum about the COM at an instant. Assuming a small perturbation, the first case uses the RZMP balancing strategy. As the perturbation increases, the second case uses the PZMP balancing strategy to minimize the rate of change in the angular momentum about the COM. For extremely strong external perturbations, the humanoid robot steps within the RHVR about the SPZMP using both the PZMP balancing strategy and tracking control for a new trajectory.

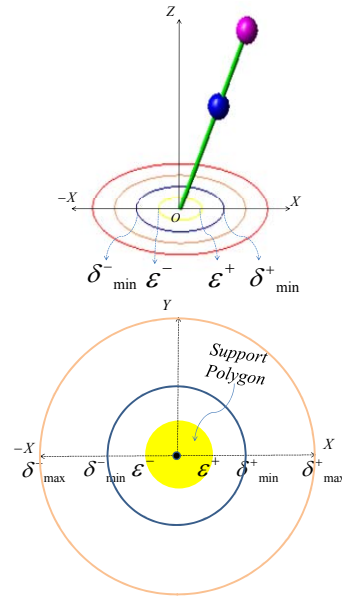


Fig. 6. RHVR of RZMP.

5.1 Case 1: RZMP balancing control

Assuming that the humanoid robot experiences a small perturbation, a RZMP balancing strategy is employed. In the LIPM, a point mass connected to a swinging leg attached to the swinging foot is maintained at a constant height and is supported by a stance foot. The effects of rotational inertia and behavior of the upper body are not considered because the upper body is approximated as a point mass at a location corresponding to a hip. Hence, control parameters are limited at the joint level.

In the RHVR about the RZMP, the range of the stability is also limited as the distance of the backward, ε^- , or forward, ε^+ , edge of the foot.

Thus,

$$\varepsilon^- < p_x^r < \varepsilon^+ \tag{68}$$

$$\therefore \varepsilon^- - \frac{z_G}{g} \ddot{x}_G < x_G < \varepsilon^+ + \frac{z_G}{g} \ddot{x}_G \tag{69}$$

The inequality (69) is the constraint of the COM about the RZMP. The linear dynamics of the LIPM from Eq. (10) can be written as

$$\begin{aligned} \ddot{x}_G &= \omega^2(x_G - p_x^r) \\ \ddot{x}_G - \omega^2 x &= f_r \end{aligned} \tag{70}$$

where $\omega = \sqrt{\frac{g}{z_G}}$ and $f_r = -\frac{g}{z_G} p_x^r$.

The solution of the differential Eq. (70) can be written as

$$x_G(t) = \left(\frac{f_r}{\omega^2} + x_0\right) \cosh(\omega t) + \frac{\dot{x}_0}{\omega} \sinh(\omega t) - \frac{f_r}{\omega^2} \tag{71}$$

5.2 Case 2: PZMP balancing control

As the perturbation increases, both the RZMP and PZMP balancing are used to minimize the rate of change in the angular momentum about the COM. In the LIDM, the maximum angular acceleration is the total sum of both the angular acceleration at the ankle point and that of the dumbbell. As compared to the LIPM, the point mass is replaced by a dumbbell to explicitly model the angular momentum about the COM. The additional angular acceleration term due to the momentum-generating dumbbell allows for a greater force. The dumbbell represents the inertia of the upper body and the swinging leg and should be subject to joint limit constraints. Thus,

$$\delta^- < p_x^p < \delta^+ \tag{72}$$

$$\delta^- - \frac{z_G}{g} \ddot{x}_G - \frac{l^2}{g} \ddot{\theta}_{i_2} < x_G < \delta^+ + \frac{z_G}{g} \ddot{x}_G + \frac{l^2}{g} \ddot{\theta}_{i_2} \tag{73}$$

The inequality (73) is the constraint of the COM about the PZMP.

This inequality represents the decision range of the PZMP. From Eq. (15), the linear dynamics of the LIDM can be written as

$$\ddot{x}_G - \omega^2 x_G = -\omega^2 (p_x^p + \frac{l^2}{g} \ddot{\theta}_{i_2}) \tag{74}$$

where $\omega = \sqrt{\frac{g}{z_G}}$ and $f_p = -\omega^2 (p_x^p + \frac{l^2}{g} \ddot{\theta}_{i_2})$.

$$x_G(t) = (\frac{f_p}{\omega^2} + x_0) \cosh(\omega t) + \frac{\dot{x}_0}{\omega} \sinh(\omega t) - \frac{f_p}{\omega^2} \tag{75}$$

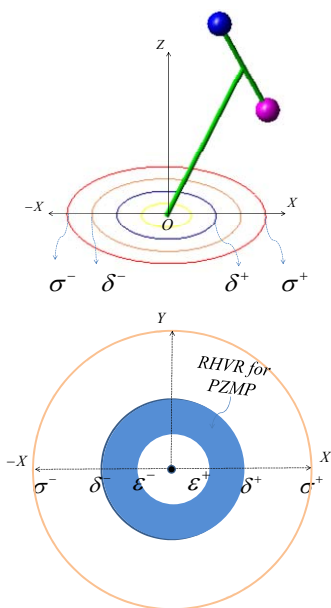


Fig. 7. RHVR of PZMP.

It appears that a minimum time control input profile can be applied for the COM angular acceleration. The COM angular acceleration profile, defined as a bang-bang trajectory, is used to generate analytical solutions.

The bang-bang function $\ddot{\theta}_{ref}(t)$ applies the maximum COM angular acceleration for a period T_1 followed by a maximum negative COM angular acceleration for a period T_2 , and finally a zero angular acceleration. The function can be written as

$$\begin{aligned} \ddot{\theta}_{ref}(t) &= \ddot{\theta}_{max} u(t) + 2\ddot{\theta}_{max} u(t-T_1) - \ddot{\theta}_{max} u(t-T_2) \\ \dot{\theta}_{ref}(t) &= \dot{\theta}_0 + \ddot{\theta}_{max} \dot{u}(t) + 2\ddot{\theta}_{max} \dot{u}(t-T_1) - \ddot{\theta}_{max} \dot{u}(t-T_2) \end{aligned} \tag{76}$$

where $\ddot{\theta}_{max}$ is the maximum angular acceleration profile until it is physically possible for the hip joint to be used and $u(t-T)$ is a unit step function at time $t=T$. $\ddot{\theta}_{ref}(t)$ is the reference angular acceleration about the dumbbell, which can cope with the COM angular acceleration generated by the external force. Assuming that $\dot{\theta}_{ref}(T_2) = \dot{\theta}_f$ and $\theta_{ref}(T_2) = \theta_{G_{i_2}}$, solving Eq. (76) gives

$$T_1 = \frac{1}{2} T_2 + \frac{1}{2\ddot{\theta}_{max}} (\dot{\theta}_f - \dot{\theta}_0) \tag{77}$$

Substituting Eq. (77) into Eq. (76), we obtain

$$(\frac{\ddot{\theta}_{max}}{4}) T_2^2 + (\frac{1}{2} (\dot{\theta}_f + \dot{\theta}_0) T_2 + (\theta_0 - \theta_{G_{i_2}} - \frac{1}{4\ddot{\theta}_{max}} (\dot{\theta}_f + \dot{\theta}_0)^2)) = 0 \tag{78}$$

Assuming $\dot{\theta}_f = \dot{\theta}_0 = 0$ and noting that $T_2 = 2T_1$, we obtain

$$\therefore T_2 = 2\sqrt{\frac{1}{\ddot{\theta}_{max}} (\theta_{G_{i_2}} - \theta_0)} \tag{79}$$

The goal of the dumbbell controller is to minimize the rate of change in the angular momentum of the COM instantaneously without exceeding the joint limit constraints. The increase in the region of stability margin in the PZMP is given by

$$\left| \frac{l^2 \ddot{\theta}_{max}}{g} \right| = |\delta^- - \epsilon^+| \tag{80}$$

The dumbbell will be controlled by methods that minimize the actual COM angular acceleration $\ddot{\theta}_{i_2}$ to move from the PZMP to the RZMP. The constraint of the PZMP can be rewritten as

$$\delta^- - \frac{\ddot{x}_G}{\omega^2} - \frac{l^2 \ddot{\theta}_{max}}{g} < x_G < \delta^+ + \frac{\ddot{x}_G}{\omega^2} + \frac{l^2 \ddot{\theta}_{max}}{g} \tag{81}$$

where $\ddot{\theta}_{max} \neq 0$.

Initially, there is a large backward angular acceleration at the dumbbell, and then, the angular acceleration is instantly reversed. The PZMP returns to the range of the RZMP.

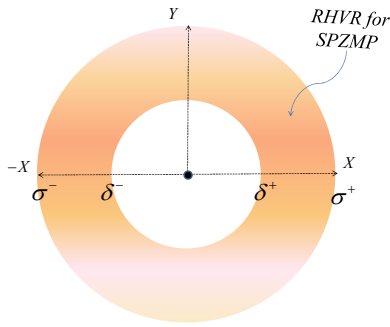


Fig. 8. RHVR for SPZMP.

5.3 Case 3: Step balancing control

When the PZMP goes lies outside the RHVR about the PZMP, the next step of the humanoid robot will be within the RHVR about the SPZMP. The dumbbell angular momentum after the external perturbation can be used to predict the horizontal components of the COM from a known ZMP trajectory. Given the ability to predict horizontal components of the COM, new reference trajectories can be generated. With specifications of walking speed and direction, the humanoid robot generates a desired gait length and period, taking into account its own morphology. Assuming that the strong perturbation can be replaced by an impulse force, resulting in an instantaneous change in the COM angular acceleration, the LIDM is very useful for predicting the resulting time evolution of the COM. The LIDM can be sufficiently complete to predict how the COM trajectories might change and to accurately determine motions for planning corrective actions that may be necessary. The RHVR for the next step location can be written by

$$\sigma^- < p_x^s < \sigma^+ \tag{82}$$

$$\sigma^- - \frac{z_G}{g} \ddot{x}_G - \frac{l^2 \ddot{\theta}_{t2}}{g} < x_G < \sigma^+ + \frac{z_G}{g} \ddot{x}_G + \frac{l^2 \ddot{\theta}_{t2}}{g}$$

where $\ddot{\theta}_{t2} \geq \ddot{\theta}_{\max}$.

The constraint gives the region of viability for the humanoid robot stepping when the angular acceleration of the COM exceeds $\ddot{\theta}_{\max}$. When there is an external perturbation, the viability control system of the humanoid robot must fundamentally change to a new control mode because the angular momentum of the COM must be minimized, and the swinging leg is located in the future step. The new control mode must minimize the additional angular momentum of the COM and track the redefined trajectory for the future step. If the RZMP lies outside the support polygon, the system must know that it will have to switch control modes instantaneously before the PZMP is located in the RHVR about the SPZMP. Thus, the system has sufficient time to switch control modes and it should compensate the changing angular acceleration of the COM and initiate a step for balance before the robot falls. The system controller then tracks the new trajectory of the swing-

ing leg and trunk the instant the actual angular momentum about the COM is minimized. Given the limitations of computational capacity, real-time trajectory planning in a joint space appears infeasible using optimization strategies with moderately long future time horizons. However, we expect the problem to be solved by the method of receding horizon control.

6. Conclusions

The contributiveness of this paper first starts from the concept that the rate of change of angular momentum generated from the center of mass is an important parameter of keeping the balance of robot, and the humanoid robot will not fall down as long as the momentum is maintained as zero. However, it is difficult to measure this momentum with sensor in the actual robot where external perturbation is working, and even more difficult to make it into zero. In this paper, the solution of inducing relatively exact momentum is suggested using Gauss’s principle. The rate of change of angular momentum generated in COM actually is predictive. Second, stable areas were divided into 3 stages by the strength of external perturbation in order to avoid robot’s fall, and such sections were defined with RHVR of each stage. The RHVR defined in each stage signifies the optimal radius of action for avoiding robot’s fall. This becomes an important criterion of proposing a solution to act upon each stage differently so that the robot may not actually fall down by external perturbation. The range definition of each stage is considered to be a method for applying realistically. We consider stability strategies for three cases. When there is a small disturbance, the RZMP balancing strategy is used. As the perturbation increases, the PZMP balancing strategy is used. The way of compensating added amount was suggested using LIDM, so that the virtual ZMP location, which is infeasible in practice, can be returned to the actual ZMP location. Finally, when there is a strong perturbation which is hard to be compensated by dumbbell, the range of robot’s step is defined, considering the mechanical limitation, both the PZMP balancing for minimizing the rate of change in the angular momentum about the COM and new trajectories of the swinging leg and trunk are applied for the SPZMP. Naturally, the new trajectory should be calculated from the desired parameters of the swinging leg within the region of the RHVR about the SPZMP. Through this, the maximum range to avoid robot’s fall was suggested. This paper does not describe how to control this in detail. Our next work will address various control issues.

Acknowledgment

This research was performed for the intelligent robotics Development Program, one of the 21st Century Frontier R&D Programs funded by the Ministry of Knowledge Economy, Republic of Korea.

References

- [1] B. Stephens, Humanoid push recovery, *The IEEE-RAS 2007 Int. Conf. Humanoid Robots*, Pittsburgh, PA, USA., (2007).
- [2] S. Kajita, F. Kanehiro, K. Kaneko, K. Yokoi and H. Hirukawa, The 3D linear inverted pendulum model: A simple modeling for a biped walking pattern generation, *Proc. of IEEE/RSJ Int. Conf. Intelligent Robots and Systems*, (2001) 239-246.
- [3] J. E. Pratt, J. Carff, S. Drakunov and A. Goswami, Capture point: A step toward humanoid push recovery, *Proc. of IEEE-RAS Int. Conf. Humanoid Robots*, (2006) 200-207.
- [4] A. Goswami, Foot rotation indicator point: A new gait planning tool to evaluate postural stability of biped robots, *Int. Conf. on Robotics and Automation*, Detroit, MI, USA., (1999) 47-52.
- [5] A. Goswami and V. Kallem, Rate of change of angular momentum and balance maintenance of biped robots, *Proc. of IEEE Int. Conf. on Robotics and Automation*, (2004) 3785-3790.
- [6] M. B. Popovic, A. Hofmann and H. Herr, Zero spot angular momentum control: Definition and applicability, *Proc. of IEEE-RAS/RSJ Int. Conf. on Humanoid Robots*, (2004) 478-493.
- [7] M. Vukobratovic, B. Borovac and D. Surdilovic, Zero moment point-Proper interpretation and new applications, *Proc. IEEE-RAS Int. Conf. Humanoid Robots*, Tokyo, Japan, (2001) 237-244.
- [8] P. Sardain and G. Bessonnet, Forces acting on a biped robot: center of pressure-zero moment point, *IEEE T. Syst. Man Cy. A*, 34 (5) (2004) 630-637.
- [9] M. Popovic, A. Goswami and H. Herr, Ground reference points in legged locomotion: Definitions, biological trajectories and control implications, *Int. J. Robo. Res.*, 24 (12) (2005) 1013-1032.
- [10] M. Popovic, A. Hofmann and H. Herr, Angular momentum regulation during human walking: biomechanics and control, *Proc. of IEEE Int. Conf. on Robotics and Automation*, New Orleans, LA, USA., (2004) 2405-2411.
- [11] F. E. Udwardia, Equations of motion for mechanical systems: A unified approach, *Int. J. Nonlinear Mech.*, 31 (1997) 951-958.
- [12] C. F. Gauss, Ueber ein neues allgemeines Grundgesetz der Mechanik (On a novel, general fundamental law for mechanics), *Journal fuer die Reine und Angewandte Mathematik (Journal of Pure and Applied mathematics)*, 4 (1829) 232-235.
- [13] F. E. Udwardia and R. E. Kalaba, On the foundations of analytical dynamics, *Int. J. Nonlinear Mech.*, 37 (2002) 1079-1090.
- [14] M. Vukobratovic and B. Borovac, Zero-moment point—Thirty-five years of its life, *Int. J. Hum. Robot.*, 1 (1) (2004) 157-173.
- [15] P. B. Wieber, On the stability of walking systems, *Proc. of Int. Workshop Humanoid and Human Friendly Robotics*, (2002).
- [16] S. Kajita, F. Kanehiro, K. Kaneko, K. Fujiwara, K. Harada, K. Yokoi and H. Hirukawa, Biped walking pattern generation by using preview control of zero-moment point, *Int. Conf. Robotics and Automation*, Taipei, Taiwan, (2003) 1620-1626.
- [17] P. B. Wieber et al., Trajectory free linear model predictive control for stable walking in the presence of strong perturbations, *Proc. of IEEE-RAS Int. Conf. Humanoid Robots*, (2006) 137-142.
- [18] J. Pratt and R. Tedrake, Velocity-based stability margins for fast bipedal walking, *First Ruperto Carola Sym. in International Science Forum of the University of Heidelberg—Fast Motions in Biomechanics and Robots*, Heidelberg, Germany, (2005).
- [19] J. E. Pratt and S. V. Drakunov, Derivation and application of a conserved orbital energy for the inverted pendulum bipedal walking model, *Proc. of the IEEE Int. Conf. Robotics and Automation*, (2007) 4653-4660.
- [20] M. Abdallah and A. Goswami, A biomechanically motivated two-phase strategy for biped upright balance control, *IEEE Int. Conf. Robotics and Automation*, (2005).
- [21] K. Hirai, M. Hirose, Y. Haikawa and T. Takenaka, The development of Honda humanoid robot, *Proc. of IEEE Int. Conf. on Robotics and Automation*, (1998) 1321-1326.
- [22] H. Herr and M. B. Popovic, Angular momentum in human walking, *J. Exp. Biol.*, 211 (2008) 467-481.
- [23] P. B. Wieber, Viability and predictive control for safe locomotion, *Proc. of IEEE/RSJ Int. Conf. on Intelligent Robots & Systems*, (2008).

Appendix

A.

The Moore–Penrose Generalized Inverse is a general method to find the solution to the following system of linear equations

$$AX = b, \quad b \in \mathbb{R}^m; X \in \mathbb{R}^n; A \in \mathbb{R}^{m \times n}$$

If the matrix A^+ satisfies all the following four conditions, the MP inverse of A is the unique matrix.

1. $AA^+A = A$
2. $A^+AA^+ = A^+$
3. $AA^+ = (AA^+)^T$
4. $A^+A = (A^+A)^T$

If A is an $m \times n$ matrix,

1. $m = n, A^+ = A^{-1}$ if A is full rank.
2. $m > n$, the solution is the one that minimizes the quantity $\|b - AX\|$.
3. $m < n$, there are infinite solutions and the MP solution is the one whose vector 2-norm is minimal.

B.

The general solution to the consistent equation $AX = b$, where A is an $m \times n$ matrix

$$X = A^+b + (I - A^+A)h,$$

where h is an $n \times 1$ vector

If an $m \times n$ matrix A has rank n ,

$$A^+ = A^T(AA^T)^+ = (A^T A)^+ A^T$$

$$A^+ = (A^T A)^{-1} A^T$$

$$(A^T A)^{-1} = (AA^T)^+$$

$$AA^+ = (A^T A)^{-1} A^T A = I$$

$$\therefore I - AA^+ = 0$$



Sangyong Lee received the B.S. degree in mechanical engineering from Chonbuk National University, JeonJu, Chonbuk, Korea, in 2000, the M.S. degree from University of Southern California, Los Angeles, USA, in 2002. He is currently a Ph.D. student in the School of Mechanical and Aerospace

Engineering at Seoul National University, Seoul, Korea. His current research interests are related to humanoid robots, dynamics & control.



Munsang Kim received the B.S. and M.S. degrees in mechanical engineering from Seoul National University, Seoul, Korea, in 1980 and 1982, respectively, and the Dr.-Ing. degree in robotics from the Technical University of Berlin, Berlin, Germany, in 1987. Since 1987, he has been a Research Scientist with the

Korea Institute of Science and Technology, Seoul, where he has led the Advanced Robotics Research Center since 2000, and became the Director of the “Intelligent Robot—The Frontier 21 Program” in October 2003. His current research interests are design and control of novel mobile manipulation systems, haptic device design and control, and sensor application to intelligent robots.



Jongwon Kim received the B.S. degree in mechanical engineering from Seoul National University, Seoul, Korea, in 1978, the M.S. degree from KAIST, Korea, in 1980, and the Ph.D. degree from the University of Wisconsin—Madison in 1987. He is currently an Associate Professor in the School of

Mechanical and Aerospace Engineering at Seoul National University in Korea. He worked as a Senior Manager at Dae-woo Heavy Industries, Ltd. His research interests are in intelligent manufacturing systems and parallel kinematic machines. Dr. Kim received the Best Paper Award from ASME Manufacturing Engineering Division in 1997 and SME University LEAD Award in 1996.



Mun-Taek Choi received his B.S., M.S. and Ph.D. degree in Aerospace and Mechanical Engineering from University of Southern California in 1994, 1997 and 2000, respectively. He is currently a Senior Research Engineer at the Center for Intelligent Robotics (Frontier 21 Program) in the Korea Institute of

Science and Technology. His research interests include software architecture for intelligent robots and dynamics & control of mechanical systems.